ENVIRONMENTAL RESEARCH
LETTERS

LETTER • OPEN ACCESS

Climate-relevant land cover composition and configuration trajectories in Europe

To cite this article: Marco Ferro *et al* 2025 *Environ. Res. Lett.* **20** 054018

ENVIRONMENTAL RESEARCH
LETTERS

CrossMark

OPEN ACCESS

RECEIVED
5 February 2025

REVISED
24 March 2025

ACCEPTED FOR PUBLICATION
3 April 2025

PUBLISHED
11 April 2025

LETTER

Climate-relevant land cover composition and configuration trajectories in Europe

Marco Ferro[1,*], Trishna Dutta[2], Silke Hüttel[3], Marcus Lindner[2], Stefan Poll[4] and Jan Börner[1,5]

1 University of Bonn, Institute for Food and Resource Economics (ILR), Bonn, Germany
2 European Forest Institute, Bonn, Germany
3 Department of Agricultural Economics and Rural Development (DARE), Georg-August-Universität Göttingen, Göttingen, Germany
4 Forschungszentrum Jülich GmbH, Institute of Bio- and Geosciences - Agrosphere (IBG-3), Jülich, Germany
5 Center for Development Research, University of Bonn, Bonn, Germany
* Author to whom any correspondence should be addressed.

E-mail: marco.ferro@ilr.uni-bonn.de

Keywords: LULCC, land cover patterns, climate change, landscape metrics, temperature

Supplementary material for this article is available online

Abstract

Land use and land cover change (LULCC) can affect the climate system by altering biophysical surface characteristics. At the local scale, climate regulating functions are co-determined by land cover composition and configuration, i.e. the proportions and the spatial arrangement of land cover types. However, research on the relationship between LULCC and climate often focuses individually either on compositional or configurational aspects. As a result, there is a gap in our knowledge about the spatiotemporal distribution of land cover composition and configuration patterns influencing the local climate regulating functions. Here, we used a range of LULCC metrics between 1992 and 2015 and applied Self-Organizing Maps to characterize dominant land cover composition and configuration trajectories in Europe. We then tested the climate relevance of the five most dominant trajectories with a high-resolution regional climate model. Land cover composition and configuration simultaneously changed in more than 20% of the European landmass, with cropland transition to forest patches and bare soil representing the major trajectory. Climate model simulations predict a general increase in the topsoil temperature due to only changes in land cover composition and configuration. All trajectories showed increasing topsoil temperature variability during the crop growing season, with forest transition trajectories showing a greater increase. Our findings demonstrate the relevance of changes in both land cover composition and configuration for the local climate and warrant further empirical and model-based research with an explicit focus on quantifying the effects of simultaneous changes in both these LULCC dimensions.

1. Introduction

Human modifications of the land cover composition and configuration through land use and land cover change (LULCC) can affect climate-regulating ecosystem functions, for instance by modifying the atmospheric water and energy cycles (Perugini *et al* 2017, Cao *et al* 2020). The land cover composition, i.e. the share of different land cover types in a given area, and the spatial land cover configuration, i.e. the way different land covers are organized in the area, are both important for the ecosystem's capacity to regulate the climate (Pielke and Avissar 1990, Pielke 2001). However, little is known about the extent and characteristics of land cover composition and configuration trajectories that may influence the ecosystem's regulating capacity. In state-of-the-art regional climate models, the typical resolution is 10–12 km (Strandberg and Lind 2021, Kostyuchenko *et al* 2022), and the sub-grid heterogeneity is represented only by land cover shares. That is, LULCC is typically represented by land cover composition without information on the spatial organization or configuration of land cover types (Rummukainen 2016, Giorgi 2019). Meanwhile, studies on land cover configuration and climate mainly focus on forest edges and microclimate, often at meter resolutions (Reinmann and Hutyra 2017, Hofmeister *et al* 2019). In the absence of considering land cover composition and configuration jointly when analyzing the net effects of LULCC on the local climate, results are likely biased and thus misinform efforts to coordinate climate mitigation and adaptation policies (Opdam *et al* 2009, Harvey *et al* 2014, Liao *et al* 2020, Peng *et al* 2021).

Previous studies using regional climate models have focused on assessing the climate signal of individual LULCC events, often in a stylized manner focusing on abrupt conversions (Rydsaa *et al* 2015, Cherubini *et al* 2018, Davin *et al* 2020); however, different LULCCs frequently occur simultaneously at the local scale. This simultaneity appears critical in the assessment of climatic effects associated with land cover patterns. For instance, evaluating the biophysical climate consequences of historical alterations in the land cover composition across Europe from 1992 to 2015, Huang *et al* (2020) observed an average temperature shift of -0.12 ± 0.20 °C at the continental scale. Yet, climate model simulations can show different temperature patterns from those in observational studies (Zhao *et al* 2013). For example, climate models predict an overall cooling effect of deforestation in mid-latitudes (Cherubini *et al* 2018, Winckler *et al* 2019), while observational studies show local warming (Alkama and Cescatti 2016, Duveiller *et al* 2018). This discrepancy may be due to the resolution of regional climate models, which may not accurately represent local climate processes driven by changes in both land cover composition and configuration.

While the effect of changes in land cover composition on temperature has been widely researched (Perugini *et al* 2017, Cao *et al* 2020), the effect of land cover configuration is still debated. Forest fragmentation is the main land cover configuration element affecting the temperature (Opdam and Wascher 2004, Decocq *et al* 2016). Under the edge effect hypothesis, increasing forest fragmentation leads to decreased moisture levels of forest patches, augmenting solar radiation with local warming as a result (Malcolm 1994, Bernaschini *et al* 2021). Contradictory, a second hypothesis postulates that forest fragmentation can in fact produce a cooling effect due to secondary circulations, such as the vegetation breeze phenomenon (Arroyo-Rodríguez *et al* 2017, Laurance *et al* 2018).

Notably, the literature on LULCC and climate adopts a broad focus on either land cover composition or configuration, leaving the effects of interactions between these two LULCC dimensions on climate insufficiently explored. In this paper, we aim to address this gap by asking: What are climate-relevant land cover composition and configuration trajectories in Europe? We rely on established LULCC metrics and a dataset able to capture climate-relevant processes for land cover composition and configuration. We employ a pattern analysis supported by machine-learning clustering to identify land cover composition and configuration trajectories between 1992 and 2015 (Levers *et al* 2018a, Sietz *et al* 2019, Zarbá *et al* 2022). We then test the climate relevance of the most dominant trajectories with a high-resolution regional climate model (Shrestha *et al* 2014).

2. Material and methods

We proceeded in two steps: First, we identified and classified common spatiotemporal patterns in land cover composition and configuration in Europe using data describing corresponding Plant Functional Types (PFTs) in 1992 and 2015. We used multiple metrics to characterize the land cover composition and configuration and Self-Organizing Maps (SOM) for multiple data layers as a clustering approach. Second, we tested the implications for the local climate of the most dominant trajectories with a high-resolution regional climate model (figure 1).

2.1. Data and resolution

We relied on land cover data from the European Space Agency Climate Change Initiative (ESA 2017), which is based on annual composites derived from satellite observations collected throughout the year. This dataset offers (1) a 300-meter spatial resolution, (2) a temporal resolution (1992–2015) that allows identifying trajectories over more than two decades coinciding with geopolitical changes that affected LULCC in Europe: the establishment of the European Union and the dissolution of the Soviet Union (Hostert *et al* 2011, Kuemmerle *et al* 2016), and (3) a land cover classification compatible with PFTs, allowing us to use the same input data for the cluster analysis and the regional climate model simulations (Smith *et al* 1993, Ustin and Gamon 2010). Using the cross-walking table provided by Li *et al* (2018) we converted the original land cover classes into 10 PFTs: (1) water and ice, (2) needleleaf evergreen forest, (3) needleleaf deciduous forest, (4) broadleaf evergreen forest, (5) broadleaf deciduous forest, (6) shrubland evergreen, (7) shrubland deciduous, (8) grassland, (9) bare soil, (10) cropland.

For the clustering analysis, we chose a grid resolution of 10×10 km because it reflects the biophysical definition of local scale provided by the International Panel on Climate Change and because it is compatible with the lower range of resolutions used in most regional climate models (Giorgi *et al* 2001, Giorgi 2019).

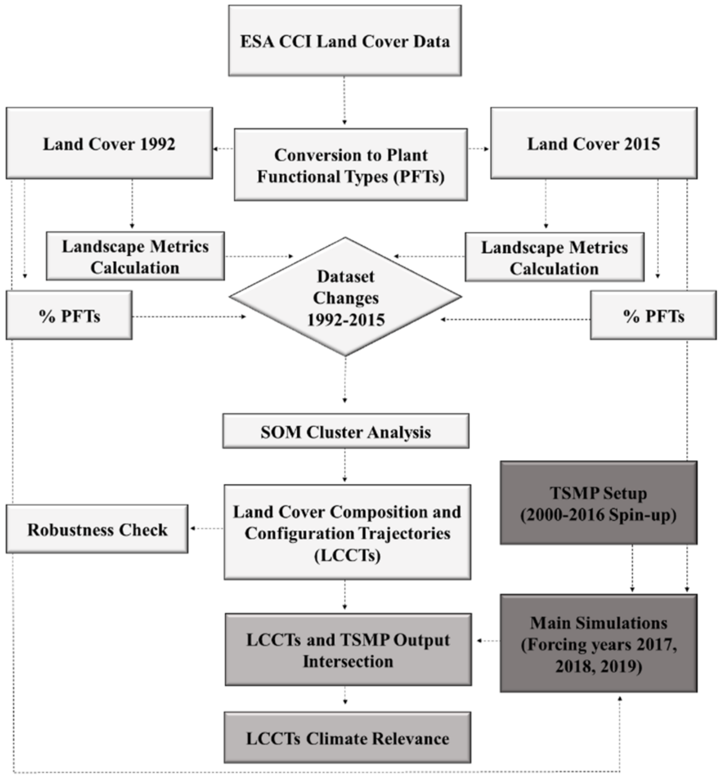

Figure 1. Flow chart of the analysis steps. The different steps are highlighted with shades of gray. In light gray the cluster analysis and in dark gray the regional climate model simulations.

2.2. LULCC metrics

To characterize land cover composition and configuration we calculated the shares of PFTs for the land cover composition and landscape metrics for the land cover configuration (Uuemaa *et al* 2009, 2013). Landscape metrics are commonly used in ecological studies to assess spatiotemporal LULCC dynamics (Smiraglia *et al* 2015, Kumar *et al* 2018) and changes in landscape fragmentation (Nagendra 2002, Llausàs and Nogué 2012). Our selection of metrics was informed by the literature and statistical criteria: We selected a pool of candidate metrics at the landscape-level from the R (R Core Team 2023) package landscapemetrics (Hesselbarth *et al* 2019). Thereby we ensured that each metric reflected a conceptual group known to be relevant in the literature, e.g. patch size, connectivity, patch shape, edge, defining a specific climate-relevant configuration aspect (Cushman *et al* 2008, Estreguil *et al* 2014, Lustig *et al* 2015). We calculated each metric from the pool at 10 × 10 km resolution using the queen´s rule, i.e. eight neighboring cells. We eliminated the metrics with a minimum 5% of missing values, for instance due to an insufficient number of land cover classes in the grid. We then removed metrics belonging to the same conceptual group based on a Spearman Correlation Index greater than 0.75 or less than −0.75 (see appendix A). This process ensured obtaining results that consistently described the main land cover configuration, and reducing redundancy to ensure results interpretation. Table 1 reports the final list of metrics, their formal definition and a description of their behavior in assessing fragmentation according to previous research (Hargis *et al* 1998, Fan and Myint 2014, Wang *et al* 2014). That is, we identified 10 variables for the shares of PFTs describing the land cover composition and 7 landscape metrics describing the land cover configuration. For brevity, a more detailed description of the utilized metrics is given in appendix A. Lastly, we calculated the variation between 1992 and 2015 for the landscape metrics and the shares of PFTs within each grid that enter the cluster analysis.

2.3. Self-organizing maps

To cluster spatiotemporal variations in land cover composition and configuration, we used an extended SOM approach for multiple data layers (Kohonen 2013). SOM is a type of neural network trained using unsupervised learning, which was originally introduced to represent high-dimensional data in a low-dimensional space. SOM is more robust in identifying homogeneous regions than hierarchical clustering or other clustering techniques, such as K-means (Lin and Chen 2006), and thus ideal for spatial data clustering purposes (Levers *et al* 2018a, van

Table 1. Selected landscape metrics used in the analysis, along with their universal component indicating the main land cover characteristic they assess, their description, and their potential effect on land cover fragmentation (Frag) derived from previous studies, where ↑ stands for increasing and ↓ for decreasing Frag.

Metric	Conceptual Group	Equation	Description	Frag
Mean of Core Area Index (CAI_MN)	Patch Size	$\mathrm{CAI_{MN}} = \frac{\sum_{i=1}^{N} \frac{CA_i}{A_i}}{N}$	CA_i = Core area of patch i A_i = Total area of patch i N= Total number of patches in the grid	↑CAI_MN ↓FRAG
Mean Shape Index (SHAPE_MN)	Patch Shape	$\mathrm{SHAPE_{MN}} = \frac{\sum_{i=1}^{N} \frac{P_i}{\sqrt{A_i}}}{N}$	P_i = Perimeter of patch i A_i = Area of patch i N= Total number of patches in the grid	↑SHAPE_MN ↑FRAG
Interspersion & Juxtaposition Index (IJI)	Connectivity	$\mathrm{IJI} = \frac{-\sum_{j=1}^{m}\sum_{k=j+1}^{m}\left[\left(\frac{e_{jk}}{E}\right)\ln\left(\frac{e_{jk}}{E}\right)\right]}{\ln(m(m-1)/2)}$	e_{jk} = Total length of edges between patch types j and k E = Total length of edges in the grid m = Number of classes in the grid	↑IJI ↓FRAG
Largest Patch Index (LPI)	Patch Size	$\mathrm{LPI} = \left(\frac{A_{\max}}{A}\right) 100$	$A_{\max}$ = Area of the largest patch in the grid A = Total grid area	↑LPI ↓FRAG
Patch Cohesion Index (COHES)	Connectivity	$\mathrm{COHES} = \left(1 - \frac{\sum_{i=1}^{n} P_i}{\sum_{i=1}^{n} P_i \sqrt{A_i}}\right) \times \left(1 - \frac{1}{\sqrt{A}}\right)^{-1} 100$	P_i = Perimeter of patch I A_i = Area of patch i N= Total number of patches in the grid A= Total grid area	↑COHES ↓FRAG
Edge Density (ED)	Edge	$\mathrm{ED} = \frac{E}{A} * 10000$	E = Total length of all edges in the grid in meters A = Total grid area in square meters	↑ED ↑FRAG
Contagion (CONTAG)	Connectivity	$\mathrm{CONTAG} = \left[1 + \sum_{i=1}^{m}\sum_{j=1}^{m} \times \left(\frac{g_{ij}}{\sum_{i=1}^{m}\sum_{j=1}^{m} g_{ij}} \ln \frac{g_{ij}}{\sum_{i=1}^{m}\sum_{j=1}^{m} g_{ij}}\right)\right] \times \frac{100}{2\ln m}$	m = Number of classes in the grid g_{ij} =Number of like adjacencies between patches of class i and j measured as the number of adjacent cell edges in the raster	↑CONTAG ↓FRAG

der Zanden *et al* 2016). Moreover, the potential of SOM for applications in Earth system science has been acknowledged in prior research (Vereecken *et al* 2016).

We applied SOM using the extension for two input layers, i.e. shares of PFTs for the composition layer and landscape metrics for the configuration layer. Equal weights were used in the training process to ensure equal importance for the two layers. We used a two-dimensional hexagonal map for the output layer and identified the optimum number of clusters K by varying the neural map dimensions from 2 × 2 to 6 × 5 and by evaluating cluster quality with the Davies–Bouldin validity index (Davies and Bouldin 1979) and the mean distance between observations and their cluster centroids (Maulik and Bandyopadhyay 2002). As shown in appendix B, the natural break point between the similarity of each cluster with its most similar other cluster and the Tanimoto distance between observations and centroids is $K = 16$ (neural map dimension 4 × 4).

The determination of the effect of the clusters on land cover fragmentation is summarized according to the behavior of metrics in table 1. The effect is assigned only when a minimum of five out of seven landscape metrics vary consistently with an increase or a decrease in landscape fragmentation. We grouped the resulting clusters into five categories based on the main compositional PFT variations. In appendix C, we also present box plots reporting additional information regarding the statistical distribution of the resulting clusters. For the clustering analysis, we used the Kohonen (Wehrens and Buydens 2007) package in R. See appendix D for additional information about the clustering algorithm, and appendix E for the labeling of the resulting clusters based on major PFT transitions.

2.4. Terrestrial systems modeling platform setup

We analyzed the effect of spatiotemporal variations in land cover composition and configuration on topsoil temperature because its variability can be directly related to local changes in atmospheric water and energy cycles, and it is preferable to air temperature when assessing climatic consequences relevant for the ecosystem functioning (Körner and Hiltbrunner 2018, Lembrechts *et al* 2022).

We used the Terrestrial Systems Modeling Platform (TerrSysMP or TSMP, https://github.com/HPSCTerrSys/TSMP). TSMP is a framework to build, setup, and run a coupled regional climate system model and works as an interface to couple component models (Shrestha *et al* 2014). We used version 1.4.0 of TSMP with a CLM3.5-COSMO5.0-OASIS3MCT component model and coupler combination (Oleson *et al* 2008, Baldauf *et al* 2011, Valcke 2013). We used a domain of 450 × 450 km, roughly corresponding to northern Germany (appendix F), where the most dominant clusters from the cluster analysis were mapped. We relied on a semi-idealized setup, simulating land cover input data in PFTs from 1992 and 2015 with atmospheric boundary forcing conditions from 2017, 2018, and 2019 ERA5 reanalysis. By holding the atmospheric-forcing constant for both land cover scenarios and calculating the differences in topsoil temperature between simulations, we isolated the climate signal attributable solely to changes in land cover composition and configuration between 1992 and 2015. The selected atmospheric forcing years represented different conditions within the domain: a wet (2017), a dry (2018), and an average year (2019), and they were selected because topsoil temperature response to LULCC might vary under different atmospheric conditions (Reshotkin and Khudyakov 2019). The grid spacing was ~3 km ($dx = dy = 0.0275$ deg) for all component models. The horizontal domain size was 150 × 150 grid points, while CLM had 10 vertical levels and COSMO had 50 respectively. The CLM time step was 3600 s while the COSMO time step was 25 s. The time span of the simulation period was the annual cycle to cover seasonal variability. We initialized the soil and land surface with a model spin-up of 17 years (2000–2016) for both land cover inputs.

3. Results

3.1. Land cover composition and configuration trajectories (LCCTs)

We identified and mapped 16 LCCTs (table 2, figure 2) between 1992 and 2015.

(1) *Stability*: The most extensive trajectory is LCCT_NC1. It accounts for nearly 75% of Europe and represents areas of stability, where very few changes in the land cover composition and configuration occurred over the 23 years. LCCT_NC2 (0.37%), located mainly in the north of Spain, did not involve changes in the land cover composition either, but the CAI_MN substantially decreased whereas CONTAG increased, which obscures the overall effect on land cover fragmentation.

(2) *Cropland Transition*: The second most extensive trajectory, LCCT_C_BS_F, covers 11.59% of Europe and indicates a transition from cropland to broadleaf deciduous forest and bare soil. This trajectory is characterized by an increase in ED and a decrease in LPI, resulting in an overall increase in land cover fragmentation. This pattern is primarily observed in Central and Eastern Europe, with a concentration in post-political-transition countries (former Soviet Union). The third most extensive trajectory, LCCT_C_BDF_G, covers 3.94% of Europe. It is characterized by a transition of cropland to broadleaf deciduous forests and grassland. In contrast to the previous trajectory, the ED decreased while CONTAG and COHES increased, leading to an overall decrease in land cover fragmentation. This pattern is predominant in the Balkan countries and parts of Southern Europe. A minor trajectory of cropland transition is LCCT_C_G, representing only 0.01% of Europe and involving the transformation of cropland to a mix of broadleaf forests and grassland.

Table 2. Land Cover Composition and Configuration Trajectories (LCCTs) spatial coverage and the mean of changes in the landscape metrics. Negative values indicate a decrease in the metric in 2015 in comparison to 1992. The effect on fragmentation is assigned when at least five out of seven landscape metrics vary consistently with their potential effect on fragmentation in table 1.

LCCTs	Category	Spatial Coverage [%]	CAI_MN	COHES	CONTAG	ED	IJI	LPI	SHAPE_MN	Frag
LCCT_NC1	Stability (74.73%)	74.36	−0.21	−0.05	0.08	−0.04	0.54	−0.33	−0.01	—
LCCT_NC2		0.37	−53.82	−0.45	94.22	0.57	0.47	−0.83	0.12	—
LCCT_C_BS_F	Cropland Transition (15.54%)	11.59	−0.32	−1.34	−6.89	1.52	1.94	−9.73	0.04	↑
LCCT_C_BDF_G		3.94	−0.02	1.70	6.04	−1.70	−0.58	10.95	−0.04	↓
LCCT_C_G		0.01	−1.24	−0.66	0.74	0.58	6.04	1.36	−0.06	—
LCCT_BDF_C_G	Forest Transition (5.33%)	2.90	0.24	−0.04	1.41	−0.62	1.46	−0.17	−0.01	↓
LCCT_NEF_G_C		2.28	0.14	−0.42	−1.23	0.59	−0.64	−4.23	0.01	↑
LCCT_NEF_SE		0.12	−0.38	1.11	2.01	0.50	−5.37	2.49	0.03	—
LCCT_BDF_BDF_G		0.03	0.40	−0.86	−2.04	0.07	2.65	−5.09	0.01	↑
LCCT_BS_NEF_G	Range Expansion (3.03%)	1.97	−0.07	1.04	7.99	−2.32	1.06	11.13	−0.07	↓
LCCT_BS_C		0.88	2.17	3.56	28.27	−6.36	−45.66	32.05	−0.11	↓
LCCT_BS_NEF		0.09	−0.06	0.81	1.95	−0.72	−1.01	3.96	0.00	—
LCCT_BS_SD_SE		0.05	−0.08	−0.65	−0.30	0.03	0.56	−1.76	0.00	↑
LCCT_BS_BEF		0.04	0.26	0.93	−0.61	−0.06	2.40	2.10	−0.03	↓
LCCT_NEF_W	Water and Ice Change (1.36%)	0.89	1.27	0.08	1.40	−1.64	0.45	−2.57	−0.02	—
LCCT_W_NEF		0.47	0.65	0.96	9.04	−1.91	−0.71	8.70	−0.07	↓

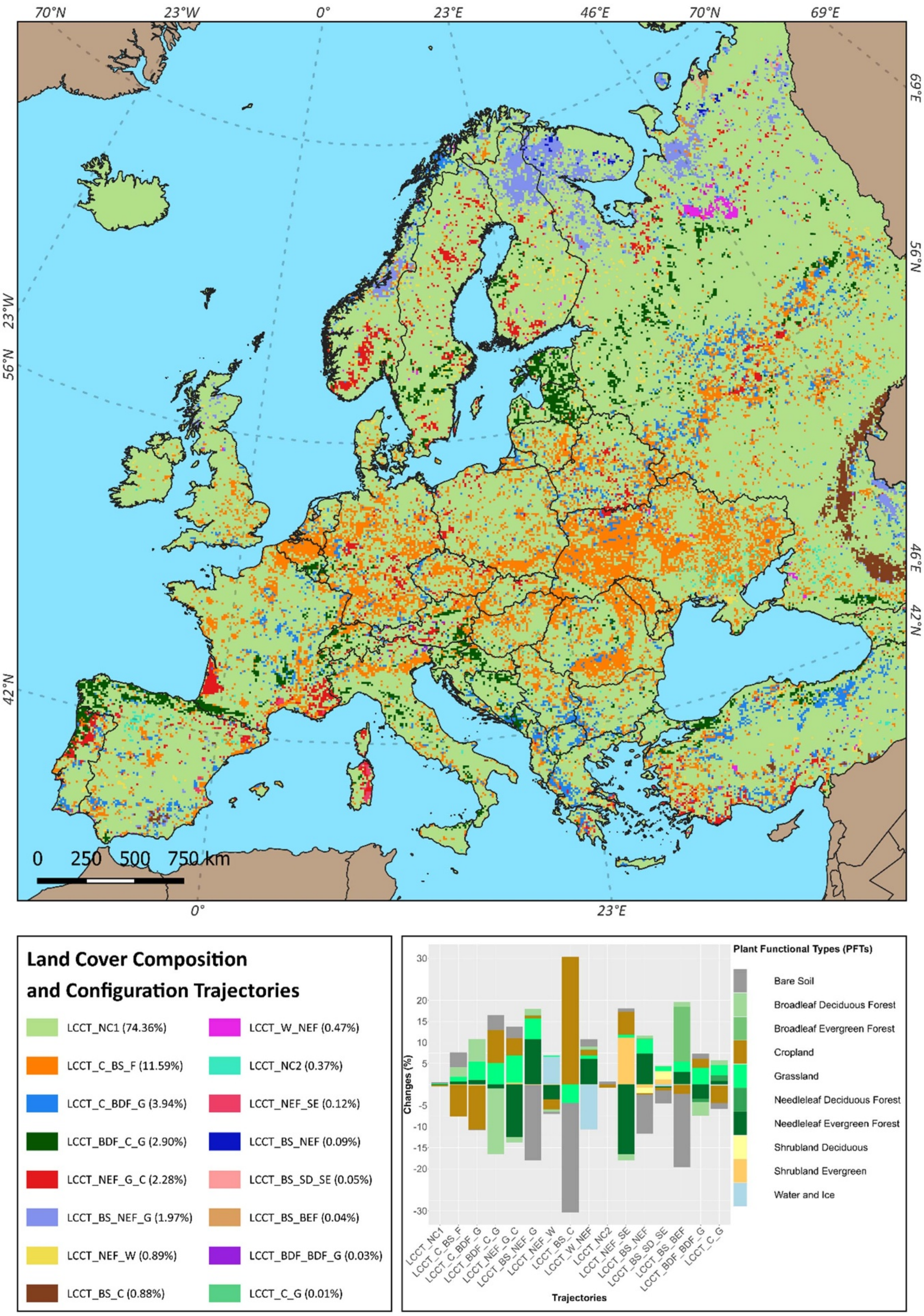

Figure 2. Land Cover Composition and Configuration Trajectories (LCCTs) between 1992 and 2015. The upper box shows the spatial distribution of the LCCTs with color schemes according to the legend in the left-bottom box. The right-bottom box displays the histogram for changes in the landscape composition; positive values indicate an expansion of the respective PFT, and negative values a contraction.

(3) *Forest Transition*: LCCT_BDF_C_G (2.90%) represents areas where broadleaf deciduous forests were converted to cropland, grassland, and bare soil. In these areas, the variation in landscape metrics implies a decrease in land cover fragmentation. We observe these changes mainly in Estonia and Latvia and the north of Spain and Portugal. LCCT_NEF_G_C (2.28%)

represents a conversion fromx needleleaf evergreen forest to grassland, cropland, and bare soil, resulting in a decrease of LPI and leading to an overall increase in land cover fragmentation. The observed pattern is concentrated predominantly in the proximity of the Aquitaine and French Alps regions in France, as well as in certain regions of Sardinia, northern Portugal, and sparsely in some areas of Northern Europe. Minor deforestation patterns are LCCT_NEF_SE (0.12%), representing changes from needleleaf evergreen forests to shrubland evergreen and cropland, and LCCT_BDF_BDF_G (0.03%) involving changes between mixed forests and grassland, cropland, and bare soil.

(4) *Range Expansion*: LCCT_BS_NEF_G, which covers 1.97% of Europe, is characterized by a revegetation process involving the conversion of bare soil to needleleaf evergreen forest and grassland. This conversion has led to an increase in LPI and CONTAG, resulting in a decrease in land cover fragmentation. This pattern is observed mainly in the north of Finland and Russia. Further revegetation trajectories have a small spatial extension. LCCT_BS_C (0.88%) represents a transition primarily from bare soil to cropland, resulting in reduced land cover fragmentation. LCCT_BS_NEF (0.09%) shows a shift from bare soil to needleleaf evergreen forest and grassland. LCCT_BS_SD_SE (0.05%) shows a change from bare soil to both deciduous and evergreen shrubland. And lastly, LCCT_BS_BEF (0.04%) represents a transformation predominantly from bare soil to broadleaf evergreen forests.

(5) *Water and Ice Change*: Trajectories involving changes in the extent of water and ice include LCCT_NEF_W (0.89%), showing the conversion from needleleaf evergreen forests and cropland to water, and LCCT_W_NEF (0.47%), showing a shift between water and ice and needleleaf evergreen forests.

To check for the ability of SOM to result in representative clusters, we calculated the distance of each grid centroid to the cluster center in the feature's space (appendix H). The result suggests that most regions were well captured by the clustering algorithm.

3.2. LCCTs climate relevance

Focusing on the five most dominant trajectories in absolute percentage (LCCT_NC1, LCCT_C_BS_F, LCCT_C_BDF_G, LCCT_BDF_C_G, LCCT_NEF_G_C), we analyzed changes in the topsoil temperature for each forcing year (2017, 2018 and 2019). By intersecting the trajectory map with regional climate model grids in the northern Germany domain, we tracked for each month the mean daily temperature variations (figure 3).

LCCT_NC1 showed relatively stable annual changes around 0.04 ± 0.21 °C (mean ± standard deviation), with summer variations (June–September) between 0.09 ± 0.19°C and -0.04 ± 0.33 °C. For LCCT_C_BS_F, annual mean temperature changes were 0.08 ± 0.18 °C in 2017, 0.05 ± 0.25 °C in 2018, and 0.04 ± 0.24 °C in 2019. During summer, the mean changes were 0.13 ± 0.23 °C in 2017, 0.04 ± 0.36 °C in 2018, and 0.03 ± 0.37 °C in 2019. LCCT_C_BDF_G showed smaller annual differences, ranging from 0.03 ± 0.21 °C in 2017 to 0.01 ± 0.27 °C in 2019, while summer differences ranged from 0.04 ± 0.29 °C to -0.03 ± 0.43 °C in 2017 and 2018, respectively. LCCT_BDF_C_G showed annual variations from 0.17 ± 0.34 °C to 0.18 ± 0.34 °C, with summer variations ranging from 0.34 ± 0.45 °C in 2019 to 0.34 ± 0.34 °C in 2017. LCCT_NEF_G_C showed an annual increase ranging from 0.15 ± 0.29 °C in 2017 to 0.17 ± 0.36 °C in 2018, and a high increase during the summer, peaking at 0.36 ± 0.48 °C in 2018. We performed a Paired Samples t-Test to statistically test daily mean differences (H0: no differences) in topsoil temperature between stability cluster LCCT_NC1 and other trajectories. Based on the testing results, we can reject the null hypothesis of no differences in daily mean topsoil temperature for all trajectories and years at any usual significance level for our study region (appendix G).

4. Discussion

Our pattern analysis using SOM reveals considerable heterogeneity in the co-occurrence of changes in the composition and configuration of Europe's land cover between 1992 and 2015. Trajectories exhibit clear variations for more than 20% of Europe. In about 14% of European landmass, land cover fragmentation increased, whereas it decreased in roughly 6%. Conversion of cropland to forest and bare soil with a consequent increase in land cover fragmentation was the main trajectory accounting for 11.59% of the total area. This trajectory was observed mainly in central-western Europe and the type of land cover transition suggests land abandonment as the main driver (Hostert *et al* 2011, Alcantara *et al* 2013). After the collapse of the Soviet Union and the establishment of the European Union, institutional, socioeconomic, and sub-optimal climatic conditions for agriculture led to outmigration from rural areas with consequent

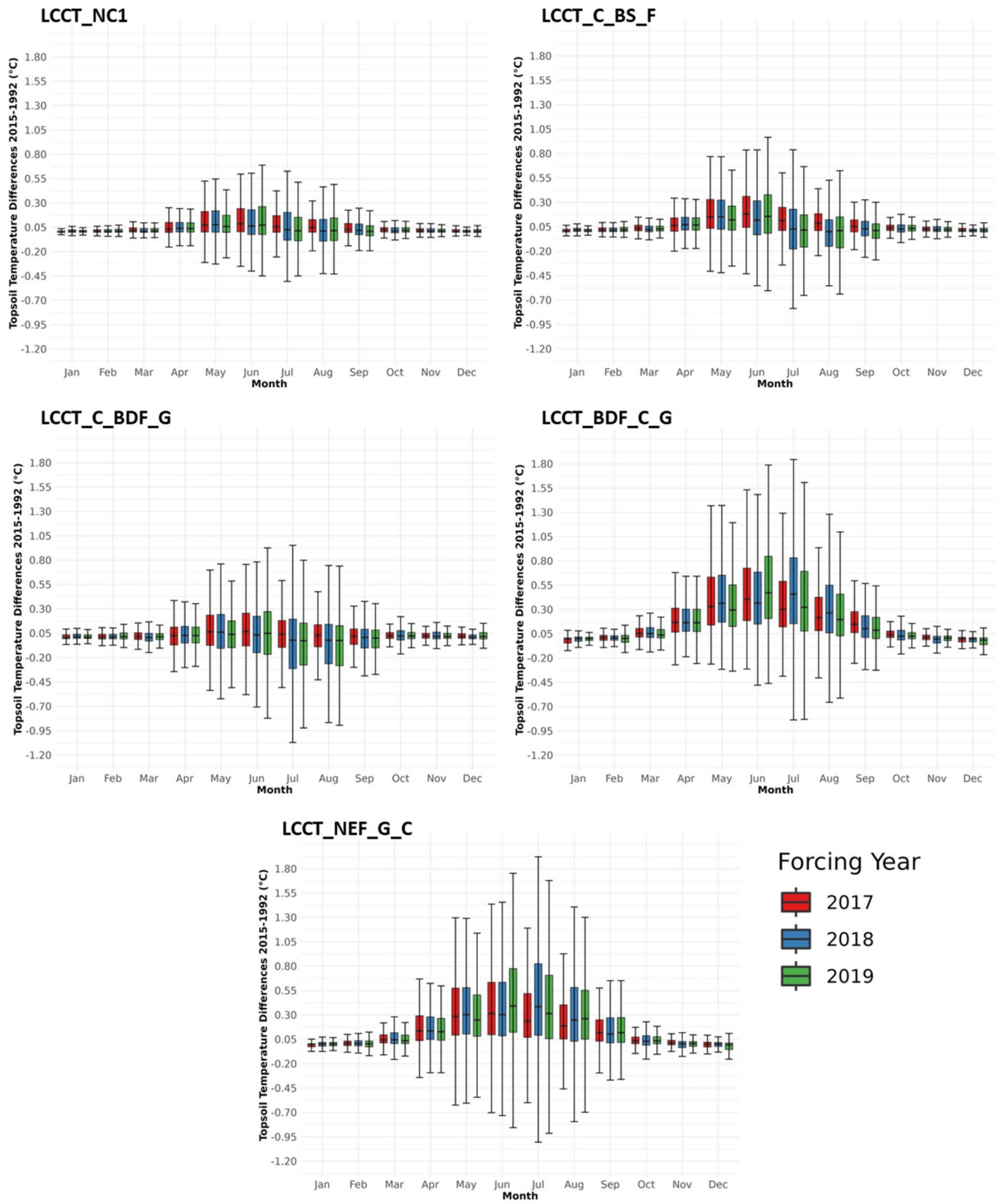

Figure 3. Box plots showing the median, the inter-quantile range, the upper and lower quantile and the whiskers of the variation (2015–1992) in the temperature for the topsoil layer only due to changes in the composition and configuration of the land cover under different atmospheric forcing conditions. The years 2017, 2018, and 2019 correspond to wet, dry, and average conditions, respectively.

abandonment of the cultivated land (Levers *et al* 2018b, Lesiv *et al* 2019).

When examining the climate relevance of the five most dominant trajectories by simulating their impact on topsoil temperature with a high-resolution regional climate model, most trajectories showed an overall topsoil temperature increase only due to land cover composition and configuration changes. Forest transition was identified as the most climate-relevant trajectory because the variations in land cover composition and configuration had the greatest impact on topsoil temperature. Furthermore, the variability of these temperature changes increased during the crop-growing season, highlighting the importance of these findings for the agricultural and forestry sectors. Increasing variability in topsoil temperature can affect crop development and yields, as well as forest root development, carbon cycling, and tree physiology. For example, it can alter the structure and function of soil microbial communities, which are critical for maintaining soil health and ecosystem processes (Wheeler *et al* 2000, Baldrian *et al* 2023).

The findings are consistent with the warming effect associated with forest transition patterns found in previous studies in northern Germany between 1992 and 2015, but inconsistent with the cooling effect associated with cropland transition (Huang *et al* 2020). In fact, in our study region, forest transition patterns have stronger warming effects compared to trajectories with increased tree cover, such as cropland transition. However, we did not observe an overall cooling effect of trees in cropland transition trajectories, but less warming compared to tree loss. These differences are likely due to the increasing complexity of the underlying mechanism driving temperature patterns when a variety of small-scale and mixed changes in land cover occur simultaneously (Huntingford *et al* 2013). One possible explanation is that, on average, cropland transition results partly in an expansion of tree cover and partly in an increase in bare soil. This suggests that the observed warming might be due to the lower albedo of bare soil, which causes warming that is not offset by increased evapotranspiration and/or secondary circulations. Another possible explanation is that the observed cropland transition increased the land cover fragmentation in the area, which may have triggered reduced moisture and increased solar radiation due to air convection (Malcolm 1994, Bernaschini *et al* 2021). In this case, the resolution of our regional climate model ($\sim$3 km)—which is higher than that used in Huang *et al* (2020) ($\sim$12 km)—more accurately represents air convection processes that are attributable to the spatial distribution and interaction of different land cover types (Prein *et al* 2015, Lucas-Picher *et al* 2021, Fosser *et al* 2024). The increase in temperature variability during summer and spring—seasons where the effects of air convection are stronger—may indicate that local surface-atmosphere interactions are more responsible for the projected warming than large-scale atmospheric circulation (Zampieri *et al* 2009, Ringard *et al* 2019). The statistically significant differences between temperatures in trajectories with few or no changes and those with more changes support this last potential explanation.

When examining the sensitivity of our results to different atmospheric forcing conditions (e.g., a wet, a dry, and an average year), we found no substantial variation in the mean daily topsoil temperature, with all years showing similar temporal patterns. This suggests that the observed temperature differences are not driven by the atmospheric forcing used in the simulations. Instead, it indicates that the effect of the trajectories on temperature remains relatively consistent under different conditions.

Overall, our findings highlight the importance of considering land cover composition and configuration simultaneously when moving beyond the typical 10–12 km resolution of regional climate models. Small-scale and mixed land cover changes can trigger processes such as air convection that are mainly influenced by changes in the land cover configuration. These processes can significantly affect climate dynamics, for example by influencing moisture levels, cloud formations, and hence incoming solar radiation, leading to differences in climate projections between studies that directly account for land cover configuration and those that do not. Additionally, our approach to classify land cover changes based on both composition and configuration metrics can help identify areas where landscape governance can implement climate mitigation and adaptation strategies by leveraging changes in both land cover aspects. Achieving this integrated perspective requires more interdisciplinary collaboration among agricultural science, forestry, ecology, and earth system science.

5. Robustness, limitations and further research needs

Spatial heterogeneity in landscape metrics depends on the spatial resolution (Wu *et al* 2002). We therefore explored scale dependency by running a comparative analysis at 15 $\times$ 15 km (appendix H). Comparing the spatial distribution and dispersion indexes, trajectories with similar attributes exhibit a robust scaling behavior between the two analyses. Nevertheless, in some cases, the SOM algorithm subdivided a cluster from the initial analysis into two or more distinct clusters in the second clustering process. Importantly, results at lower resolution were similar to our initial findings.

As any empirical study, ours comes with some limitations: First, given that we compare land cover realities at two points in time, LULCC dynamics that involve regular patterns, such as crop-tree rotations and fallows, may not be appropriately captured by our approach. Previous investigations showed that dominant LULCC trajectories last on average 14 years (Crawford *et al* 2022), and a significant proportion of LULCC in Europe can be attributed to geopolitical shifts in the 1990s (Kuemmerle *et al* 2016), a timeframe adequately covered by our analysis. Second, our assessment of how the identified land cover trajectories affect the local climate may obey limited external validity. And third, our regional climate model may not yet be able to capture all relevant processes occurring at higher resolution.

Further research is needed to (1) better understand the underlying mechanisms driving temperature changes at the local scale when land cover composition and configuration change simultaneously, (2) predict potential future implications for the regional climate, agriculture, and forestry, and (3) inform decision-makers about politically feasible policy options (e.g., afforestation strategies) to make European land systems more resilient to a warming climate.

Data availability statement

The data that support the findings of this study are openly available at the following URL/DOI: https://doi.org/10.5281/zenodo.14811573. Additional data and code are available from the corresponding author upon request.

Acknowledgments

The authors gratefully acknowledge financial support from the Deutsche Forschungsgemeinschaft (DFG, German Research Foundation)—SFB 1502/1–2022—Project Number: 450058266.

The authors gratefully acknowledge the Gauss Centre for Supercomputing e.V. (www.gauss-centre.eu) for funding this project by providing computing time through the John von Neumann Institute for Computing (NIC) on the GCS Supercomputer JUWELS at Jülich Supercomputing Centre (JSC).

Conflict of interest

The authors declare no competing interests.

ORCID iDs

Marco Ferro https://orcid.org/0009-0002-5020-3044
Trishna Dutta https://orcid.org/0000-0002-5236-2658
Silke Hüttel https://orcid.org/0000-0002-2141-2931
Marcus Lindner https://orcid.org/0000-0002-0770-003X
Stefan Poll https://orcid.org/0000-0003-2527-0747
Jan Börner https://orcid.org/0000-0003-3034-5360

References

Alcantara C *et al* 2013 Mapping the extent of abandoned farmland in Central and Eastern Europe using MODIS time series satellite data *Environ. Res. Lett.* **8** 035035

Alkama R and Cescatti A 2016 Biophysical climate impacts of recent changes in global forest cover *Science* **351** 600–4

Arroyo-Rodríguez V, Saldaña-Vázquez R A, Fahrig L and Santos B A 2017 Does forest fragmentation cause an increase in forest temperature? *Ecol. Res.* **32** 81–88

Baldauf M, Seifert A, Förstner J, Majewski D, Raschendorfer M and Reinhardt T 2011 Operational convective-scale numerical weather prediction with the COSMO model: description and Sensitivities (available at: https://journals.ametsoc.org/view/journals/mwre/139/12/mwr-d-10-05013.1.xml)

Baldrian P, López-Mondéjar R and Kohout P 2023 Forest microbiome and global change *Nat. Rev. Microbiol.* **21** 487–501

Bernaschini M L, Rossetti M R, Valladares G and Salvo A 2021 Microclimatic edge effects in a fragmented forest: disentangling the drivers of ecological processes in plant–leafminer–parasitoid food webs *Ecol. Entomol.* **46** 1047–58

Cao Q, Liu Y, Georgescu M and Wu J 2020 Impacts of landscape changes on local and regional climate: a systematic review *Landscape Ecol.* **35** 1269–90

Cherubini F, Huang B, Hu X, Tölle M H and Strømman A H 2018 Quantifying the climate response to extreme land cover changes in Europe with a regional model *Environ. Res. Lett.* **13** 074002

Crawford C L, Yin H, Radeloff V C and Wilcove D S 2022 Rural land abandonment is too ephemeral to provide major benefits for biodiversity and climate *Sci. Adv.* **8** eabm8999

Cushman S A, McGarigal K and Neel M C 2008 Parsimony in landscape metrics: strength, universality, and consistency *Ecol. Indic.* **8** 691–703

Davies D L and Bouldin D W 1979 A cluster separation measure *IEEE Trans. Pattern Anal. Mach. Intell.* **PAMI-1** 224–7

Davin E L *et al* 2020 Biogeophysical impacts of forestation in Europe: first results from the LUCAS (Land Use and Climate Across Scales) regional climate model intercomparison *Earth Syst. Dyn.* **11** 183–200

Decocq G *et al* 2016 Ecosystem services from small forest patches in agricultural landscapes *Curr. For. Rep.* **2** 30–44

Duveiller G, Hooker J and Cescatti A 2018 The mark of vegetation change on Earth's surface energy balance *Nat. Commun.* **9** 679

ESA 2017 Land cover CCI product user guide version 2 *Tech. Rep.* (available at: maps.elie.ucl.ac.be/CCI/viewer/download/ESACCI-LC-Ph2-PUGv2_2.0.pdf)

Estreguil C, de Rigo D and Caudullo G 2014 A proposal for an integrated modelling framework to characterise habitat pattern *Environ. Model. Softw.* **52** 176–91

Fan C and Myint S 2014 A comparison of spatial autocorrelation indices and landscape metrics in measuring urban landscape fragmentation *Landscape Urban Plan.* **121** 117–28

Fosser G *et al* 2024 Convection-permitting climate models offer more certain extreme rainfall projections *npj Clim. Atmos. Sci.* **7** 1–10

Giorgi F 2019 Thirty years of regional climate modeling: where are we and where are we going next? *J. Geophys. Res. Atmos.* **124** 5696–723

Giorgi F *et al* 2001 Regional climate information- evaluation and projections *Climate Change 2001: The Scientific Basis. Contribution of Working Group to the Third Assessment Report of the Intergouvernmental Panel on Climate Change* ed J T Houghton *et al* (Cambridge University Press) (available at: https://epic.awi.de/id/eprint/4973/)

Hargis C D, Bissonette J A and David J L 1998 The behavior of landscape metrics commonly used in the study of habitat fragmentation *Landscape Ecol.* **13** 167–86

Harvey C A *et al* 2014 Climate–smart landscapes: opportunities and challenges for integrating adaptation and mitigation in tropical agriculture *Conserv. Lett.* **7** 77–90

Hesselbarth M H K, Sciaini M, With K A, Wiegand K and Nowosad J 2019 landscapemetrics : an open–source R tool to calculate landscape metrics *Ecography* **42** 1648–57

Hofmeister J, Hošek J, Brabec M, Střalková R, Mýlová P, Bouda M, Pettit J L, Rydval M and Svoboda M 2019 Microclimate edge effect in small fragments of temperate forests in the context of climate change *For. Ecol. Manage.* **448** 48–56

Hostert P, Kuemmerle T, Prishchepov A, Sieber A, Lambin E F and Radeloff V C 2011 Rapid land use change after socio-economic disturbances: the collapse of the Soviet Union versus Chernobyl *Environ. Res. Lett.* **6** 045201
Huang B, Hu X, Fuglstad G-A, Zhou X, Zhao W and Cherubini F 2020 Predominant regional biophysical cooling from recent land cover changes in Europe *Nat. Commun.* **11** 1066
Huntingford C *et al* 2013 Simulated resilience of tropical rainforests to CO_2-induced climate change *Nat. Geosci.* **6** 268–73
Kohonen T 2013 Essentials of the self-organizing map *Neural Netw.* **37** 52–65
Körner C and Hiltbrunner E 2018 The 90 ways to describe plant temperature *Perspect. Plant Ecol. Evol. Syst.* **30** 16–21
Kostyuchenko Y, Artemenko I, Abioui M and Benssaou M 2022 Global and regional climatic modeling *Encyclopedia of Mathematical Geosciences* (*Encyclopedia of Earth Sciences Series*) ed B S Daya Sagar, Q Cheng, J McKinley and F Agterberg (Springer) pp 1–5
Kuemmerle T *et al* 2016 Hotspots of land use change in Europe *Environ. Res. Lett.* **11** 064020
Kumar M, Denis D M, Singh S K, Szabó S and Suryavanshi S 2018 Landscape metrics for assessment of land cover change and fragmentation of a heterogeneous watershed *Remote Sens. Appl.* **10** 224–33
Laurance W F, Camargo J L C, Fearnside P M, Lovejoy T E, Williamson G B, Mesquita R C G, Meyer C F J, Bobrowiec P E D and Laurance S G W 2018 An Amazonian rainforest and its fragments as a laboratory of global change *Biol. Rev. Camb. Phil. Soc.* **93** 223–47
Lembrechts J J *et al* 2022 Global maps of soil temperature *Glob. Change Biol.* **28** 3110–44
Lesiv M *et al* 2019 Estimating the global distribution of field size using crowdsourcing *Glob. Change Biol.* **25** 174–86
Levers C *et al* 2018a Archetypical patterns and trajectories of land systems in Europe *Reg. Environ. Change* **18** 715–32
Levers C, Schneider M, Prishchepov A V, Estel S and Kuemmerle T 2018b Spatial variation in determinants of agricultural land abandonment in Europe *Sci. Total Environ.* **644** 95–111
Li W, MacBean N, Ciais P, Defourny P, Lamarche C, Bontemps S, Houghton R A and Peng S 2018 Gross and net land cover changes in the main plant functional types derived from the annual ESA CCI land cover maps (1992–2015) *Earth Syst. Sci. Data* **10** 219–34
Liao C *et al* 2020 Advancing landscape sustainability science: theoretical foundation and synergies with innovations in methodology, design, and application *Landscape Ecol.* **35** 1–9
Lin G-F and Chen L-H 2006 Identification of homogeneous regions for regional frequency analysis using the self-organizing map *J. Hydrol.* **324** 1–9
Llausàs A and Nogué J 2012 Indicators of landscape fragmentation: the case for combining ecological indices and the perceptive approach *Ecol. Indic.* **15** 85–91
Lucas-Picher P, Argüeso D, Brisson E, Tramblay Y, Berg P, Lemonsu A, Kotlarski S and Caillaud C 2021 Convection-permitting modeling with regional climate models: latest developments and next steps *WIREs Clim. Change* **12** e731
Lustig A, Stouffer D B, Roigé M and Worner S P 2015 Towards more predictable and consistent landscape metrics across spatial scales *Ecol. Indic.* **57** 11–21
Malcolm J R 1994 Edge effects in central Amazonian forest fragments *Ecology* **75** 2438
Maulik U and Bandyopadhyay S 2002 Performance evaluation of some clustering algorithms and validity indices *IEEE Trans. Pattern Anal. Mach. Intell.* **24** 1650–4
Nagendra H 2002 Opposite trends in response for the Shannon and Simpson indices of landscape diversity *Appl. Geogr.* **22** 175–86
Oleson K W *et al* 2008 Improvements to the Community Land Model and their impact on the hydrological cycle *J. Geophys. Res.* **113** G01021
Opdam P, Luque S and Jones K B 2009 Changing landscapes to accommodate for climate change impacts: a call for landscape ecology *Landscape Ecol.* **24** 715–21
Opdam P and Wascher D 2004 Climate change meets habitat fragmentation: linking landscape and biogeographical scale levels in research and conservation *Biol. Conserv.* **117** 285–97
Peng J, Liu Y, Corstanje R and Meersmans J 2021 Promoting sustainable landscape pattern for landscape sustainability *Landscape Ecol.* **36** 1839–44
Perugini L, Caporaso L, Marconi S, Cescatti A, Quesada B, de Noblet-ducoudré N, House J I and Arneth A 2017 Biophysical effects on temperature and precipitation due to land cover change *Environ. Res. Lett.* **12** 053002
Pielke R A 2001 Influence of the spatial distribution of vegetation and soils on the prediction of cumulus Convective rainfall *Rev. Geophys.* **39** 151–77
Pielke R A and Avissar R 1990 Influence of landscape structure on local and regional climate *Landscape Ecol.* **4** 133–55
Prein A F *et al* 2015 A review on regional convection-permitting climate modeling: demonstrations, prospects, and challenges *Rev. Geophys.* **53** 323–61
R Core Team 2023 R: a language and environment for statistical computing (available at: www.R-project.org/)
Reinmann A B and Hutyra L R 2017 Edge effects enhance carbon uptake and its vulnerability to climate change in temperate broadleaf forests *Proc. Natl Acad. Sci. USA* **114** 107–12
Reshotkin O V and Khudyakov O I 2019 Soil temperature response to modern climate change at four sites of different latitude in the European part of Russia *IOP Conf. Ser.: Earth Environ. Sci.* **368** 012040
Ringard J, Chiriaco M, Bastin S and Habets F 2019 Recent trends in climate variability at the local scale using 40 years of observations: the case of the Paris region of France *Atmos. Chem. Phys.* **19** 13129–55
Rummukainen M 2016 Added value in regional climate modeling *WIREs Clim. Change* **7** 145–59
Rydsaa J H, Stordal F and Tallaksen L M 2015 Sensitivity of the regional European boreal climate to changes in surface properties resulting from structural vegetation perturbations *Biogeosciences* **12** 3071–87
Shrestha P, Sulis M, Masbou M, Kollet S and Simmer C 2014 A scale-consistent terrestrial systems modeling platform based on COSMO, CLM, and PARFLOW (available at: https://journals.ametsoc.org/view/journals/mwre/142/9/mwr-d-14-00029.1.xml)
Sietz D, Frey U, Roggero M, Gong Y, Magliocca N, Tan R, Janssen P and Václavík T 2019 Archetype analysis in sustainability research: methodological portfolio and analytical frontiers *Ecol. Soc.* **24** 18
Smiraglia D, Ceccarelli T, Bajocco S, Perini L and Salvati L 2015 Unraveling landscape complexity: land use/land cover changes and landscape pattern dynamics (1954–2008) in contrasting peri-urban and agro-forest regions of Northern Italy *Environ. Manage.* **56** 916–32
Smith T M, Shugart H H, Woodward F I and Burton P J 1993 Plant functional types *Vegetation Dynamics & Global Change* (Springer) pp 272–92
Strandberg G and Lind P 2021 The importance of horizontal model resolution on simulated precipitation in Europe—from global to regional models *Weather Clim. Dyn.* **2** 181–204
Ustin S L and Gamon J A 2010 Remote sensing of plant functional types *New Phytol.* **186** 795–816
Uuemaa E, Antrop M, Roosaare J, Marja R and Ü M 2009 Landscape metrics and indices: an overview of their use in landscape research *Living Rev. Landscape Res.* **3** 1–28
Uuemaa E, Mander Ü and Marja R 2013 Trends in the use of landscape spatial metrics as landscape indicators: a review *Ecol. Indic.* **28** 100–6
Valcke S 2013 The OASIS3 coupler: a European climate modelling community software *Geosci. Model Dev.* **6** 373–88

van der Zanden E H, Levers C, Verburg P H and Kuemmerle T 2016 Representing composition, spatial structure and management intensity of European agricultural landscapes: a new typology *Landscape Urban Plan.* **150** 36–49

Vereecken H, Pachepsky Y, Simmer C, Rihani J, Kunoth A, Korres W, Graf A, Franssen H J-H, Thiele-Eich I and Shao Y 2016 On the role of patterns in understanding the functioning of soil-vegetation-atmosphere systems *J. Hydrol.* **542** 63–86

Wang X, Blanchet F G, Koper N and Tatem A 2014 Measuring habitat fragmentation: an evaluation of landscape pattern metrics *Methods Ecol. Evol.* **5** 634–46

Wehrens R and Buydens L M C 2007 Self- and super-organizing maps in R : the kohonen package *J. Stat. Softw.* **21** 1–19

Wheeler T R, Craufurd P Q, Ellis R H, Porter J R and Vara Prasad P V 2000 Temperature variability and the yield of annual crops *Agric. Ecosyst. Environ.* **82** 159–67

Winckler J, Reick C H, Luyssaert S, Cescatti A, Stoy P C, Lejeune Q, Raddatz T, Chlond A, Heidkamp M and Pongratz J 2019 Different response of surface temperature and air temperature to deforestation in climate models *Earth Syst. Dyn.* **10** 473–84

Wu J, Shen W, Sun W and Tueller P T 2002 Empirical patterns of the effects of changing scale on landscape metrics *Landscape Ecol.* **17** 761–82

Zampieri M, D'Andrea F, Vautard R, Ciais P, de Noblet-ducoudré N and Yiou P 2009 Hot European summers and the role of soil moisture in the propagation of mediterranean drought *J. Clim.* **22** 4747–58

Zarbá L *et al* 2022 Mapping and characterizing social-ecological land systems of South America *Ecol. Soc.* **27** 27

Zhao L, Xu J and Powell A M Jr 2013 Discrepancies of surface temperature trends in the CMIP5 simulations and observations on the global and regional scales *Clim. Past Dis.* **9** 6161–78